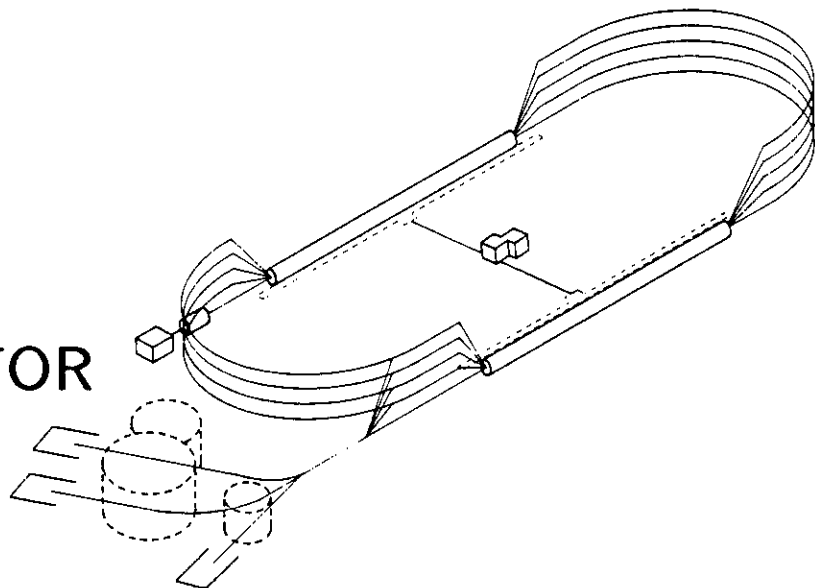


CEBAF PR-93--029
JUNE 1993

Integrated Numerical Modeling of a Laser Gun Injector

*H. Liu, S. Benson, J. Bisognano, P. Liger, G. Neil, D. Neuffer,
C. Sinclair, and B. Yunn
Continuous Electron Beam Accelerator Facility
12000 Jefferson Avenue
Newport News, VA 23606*

CONTINUOUS
ELECTRON
BEAM
ACCCELERATOR
FACILITY



SURA SOUTHEASTERN UNIVERSITIES RESEARCH ASSOCIATION

CEBAF

Newport News, Virginia

Copies available from:

Library
CEBAF
12000 Jefferson Avenue
Newport News
Virginia 23606

The Southeastern Universities Research Association (SURA) operates the Continuous Electron Beam Accelerator Facility for the United States Department of Energy under contract DE-AC05-84ER40150.

DISCLAIMER

This report was prepared as an account of work sponsored by the United States government. Neither the United States nor the United States Department of Energy, nor any of their employees, makes any warranty, express or implied, or assumes any legal liability or responsibility for the accuracy, completeness, or usefulness of any information, apparatus, product, or process disclosed, or represents that its use would not infringe privately owned rights. Reference herein to any specific commercial product, process, or service by trade name, mark, manufacturer, or otherwise, does not necessarily constitute or imply its endorsement, recommendation, or favoring by the United States government or any agency thereof. The views and opinions of authors expressed herein do not necessarily state or reflect those of the United States government or any agency thereof.

Integrated Numerical Modeling of a Laser Gun Injector *

H. Liu, S. Benson, J. Bisognano, P. Liger, G. Neil, D. Neuffer, C. Sinclair and B. Yunn
CEBAF, 12000 Jefferson Ave., Newport News, VA 23606

Abstract

CEBAF is planning to incorporate a laser gun injector into the linac front end as a high-charge cw source for a high-power free electron laser and nuclear physics. This injector consists of a DC laser gun, a buncher, a cryounit and a chicane. The performance of the injector is predicted based on integrated numerical modeling using POISSON, SUPERFISH and PARMELA. The point-by-point method incorporated into PARMELA by McDonald is chosen for space charge treatment. The concept of "conditioning for final bunching" is employed to vary several crucial parameters of the system for achieving highest peak current while maintaining low emittance and low energy spread. Extensive parameter variation studies show that the design will perform beyond the specifications for FEL operations aimed at industrial applications and fundamental scientific research. The calculation also shows that the injector will perform as an extremely bright cw electron source.

I. INTRODUCTION

CEBAF has been studying an IR FEL and a UV FEL utilizing the superconducting accelerator technology that has been developed at CEBAF, aimed at industrial applications and fundamental scientific research[1-4]. An FEL injector based on a DC laser gun will be used as a high-brightness cw source. The schematic of the injector is shown in Fig. 1. The DC laser gun produces a cw train of electron bunches at 400 ~ 500 keV with bunch lengths of 60 ~ 100 ps. Then electrons are bunched using a room-temperature buncher to provide suitable injection into a cryounit containing two standard CEBAF SRF cavities. The cryounit accelerates the electrons up to ~ 10 MeV while providing suitable tilt in longitudinal phase space distributions. Then the electrons are finally bunched using a chicane with a $R_{56} = 0.085$ cm/%.

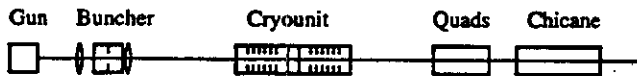


Fig. 1 Schematic of the FEL injector

The specifications for our FEL injector are summarised in Table 1. Throughout the paper, the bunch length and energy spread are represented using $4\sigma_z$ and $4\sigma_E$, which correspond to 95% particles for ideal Gaussian distributions. For non-Gaussian distributions, they generally still correspond to ~ 90% particles.

*Supported by Virginia Center for Innovative Technology

Table 1 FEL Injector Specifications

Energy	10 MeV
Charge per bunch	120 pC
Bunch length ($4\sigma_z$)	2 ps
Energy spread ($4\sigma_E$)	400 keV
Normalised rms emittance (ϵ_n)	15 mm mrad
Average beam current	900 μ A
Repetition frequency	7.677 MHz

In this paper, we present our injector performance predictions based on integrated numerical modeling using POISSON, SUPERFISH and PARMELA.

II. CHICANE BUNCHING

Chicane bunching is not a new method for compressing electrons, and it has been clearly described, e.g., in Ref. 5. However, as will be shown later in this paper, it fits our injector design quite well when it is used together with two standard CEBAF SRF cavities. Therefore we introduce this bunching mechanism first instead of going to the numerical results immediately.

The bunching process using a chicane with two SRF cavities in our injector design is shown in Fig. 2. Using the

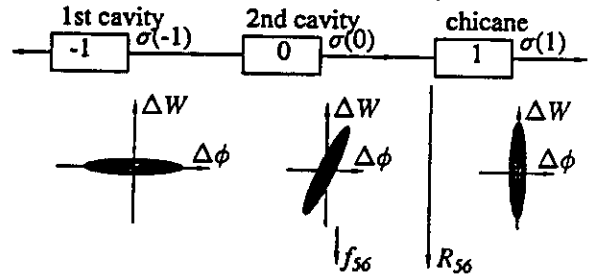


Fig. 2 Bunching using a chicane with two SRF cavities
standard σ matrix representation, we have the following mathematical description

$$\sigma_{55}(1) = \sigma_{55}(0)(1 - R_{56}/f_{56})^2 + R_{56}^2\sigma_{66}(-1),$$

where $\sqrt{\sigma_{55}(0)}$ is the bunch length at the entrance of the chicane, $\sqrt{\sigma_{55}(1)}$ the bunch length at the exit of the chicane, $\sqrt{\sigma_{66}(-1)}$ the momentum spread at the entrance of the second SRF cavity, $R_{56} = \delta l / (\delta p/p)$ the parameter of the bunching property of the chicane, δl the path difference between electrons having an energy spread of

$\delta p/p$, and $f_{56} = -\sigma_{56}(0)/\sigma_{56}(0)$ the tilt of the longitudinal phase space distribution of the bunch at the exit of the second SRF cavity. It is seen that when $f_{56} \simeq R_{56}$, the final bunch length depends only on the product of the momentum spread and R_{56} of the chicane. We call the above condition the *conditioning for final bunching*, which is a term borrowed from Ref. 6. It has been built into PARMELA so that f_{56} can be calculated statistically from all the particles at the exits of the SRF cavities, and by comparison with R_{56} of the chicane, the matching of longitudinal phase space distributions from the second SRF cavity to the chicane can be accurately predicted accordingly. This has turned out to be an indispensable means for optimizing the design efficiently.

III. NUMERICAL MODELING

Based on the previous calculation[4], the performance of the FEL injector has been thoroughly investigated and optimised using time-consuming but accurate integrated numerical modeling. The beam dynamics is calculated using a version of PARMELA with the point-by-point method for space charge treatment[7,8]. The code POISSON was used to generate the DC electrical fields in the photocathode gun, and the code SUPERFISH was used to generate the 2-D RF fields in the buncher and two SRF cavities in the cryounit. In each integrated simulation (~ 10 cpu-hours on an HP 9000/730 UNIX workstation), the same electrons are followed from emission at the photocathode through the gun, the buncher, the cryounit and the chicane.

a) Baseline Design

The injector performance was optimized at first for the baseline design which corresponds to 500 kV gun voltage, 100 ps laser pulse length and 3 mm cathode diameter. The distance from the gun to the buncher is reduced to account for the divergence (~ 20 mrad) of the beam out of the gun, and the distance from the buncher to the cryounit is increased to meet the optimum bunching requirement. The performance of the baseline design is shown in Table 2. It is seen that the injector performance stays well within the specifications by a factor of 2 \sim 3. Various distributions of the bunch are shown in Fig. 3.

Table 2 Performance of the Baseline Design

Bunch charge	120 pC
Bunch length ($4\sigma_t$)	0.96 ps
Energy spread ($4\sigma_E$)	290 keV
Mean energy (E_m)	9.492 MeV
Norm. rms emit. ($\epsilon_{ns}/\epsilon_{ny}$)	4.44/4.73 (mm mrad)

b) Robustness of the Baseline Design

The robustness of the baseline design has been investigated against the laser intensity fluctuation and so the bunch charge fluctuation. A series of integrated simulations were conducted with all the system parameters fixed

while the bunch charge was varied from 120 pC to 160 pC. The variations of the bunch performance at the exit of

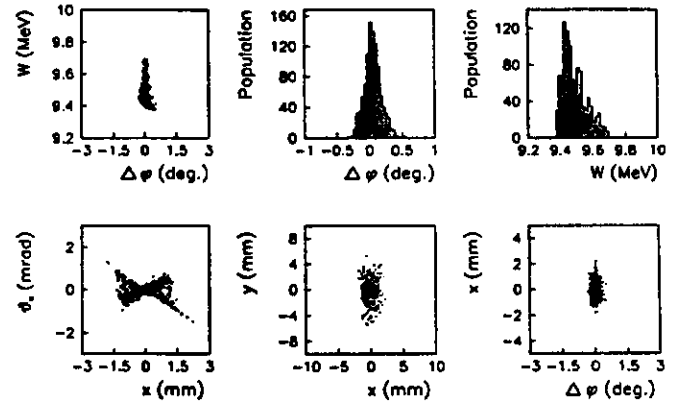


Fig. 3 Various distributions of 1000 superparticles at the exit of the chicane, showing the optimized baseline design performance listed in Table 2. *upper left*: longitudinal phase space distribution (W - energy; $\Delta\phi$ - relative phase); *upper middle*: phase profile; *upper right*: energy profile; *lower left*: horizontal trace space distribution (x - horizontal position; θ_x - horizontal divergence angle); *lower middle*: cross-sectional distribution; *lower right*: horizontal snapshot.

the chicane are listed in Table 3, where δE_m and $\delta\phi_m$ represent the mean energy shift and the phase shift of the bunch centroid. The units are pC for bunch charge, ps for bunch length, keV for energy spread, mm mrad for emittance, keV and degree for centroidal energy and phase shifts throughout the paper. It is seen that the mean energy shift and the phase shift of the bunch centroid caused by the charge fluctuations are negligible.

Table 3 Robustness of the Baseline Design

Q	$4\sigma_t$	$4\sigma_E$	$\epsilon_{ns}/\epsilon_{ny}$	δE_m	$\delta\phi_m$
120	0.96	290	4.44/4.73	0	0 (baseline)
140	1.04	281	4.99/5.31	-1	-0.0048
150	1.11	277	5.25/5.58	-1	-0.0075
155	1.17	275	5.37/5.71	-2	-0.0092
160	1.21	273	5.50/5.84	-2	-0.0092

c) Sensitivity of the Baseline Design

The sensitivity of the baseline design has been investigated on the basis of $\delta\phi = \pm 2^\circ$ for the RF phase change and $\delta E/E = \pm 2\%$ for the RF amplitude change in the buncher and the two RF cavities in the cryounit. For each case only one parameter was varied with all the others being the same as for the optimized baseline design stated in Table 2. The results are listed in Table 4. It is found that the most sensitive performance is the bunch length. The most sensitive system parameters, in sequence, are the RF phase of the second SRF cavity, the RF amplitude

of the second SRF cavity, the RF amplitude of the first SRF cavity and the RF phase of the first SRF cavity. The sensitivity comes from the resultant mean energy shift of the particles and the small value of R_{66} of the chicane. However, no case is found to be out of the specifications.

Table 4 Sensitivity of the Baseline Design

<i>Element</i>	$\delta\phi$	$\delta E/E$	$4\sigma_L$	$4\sigma_E$	$\epsilon_{nz}/\epsilon_{ny}$	δE_m	$\delta\phi_m$
(Baseline)	0.0	0.0	0.96	290	4.44/4.73	0.0	0.0
Buncher	+2	0.0	1.57	306	4.69/4.98	-51	+0.42
Buncher	-2	0.0	1.37	261	4.23/4.50	+56	-0.47
Buncher	0.0	+2	1.05	309	4.52/4.81	-1	+0.025
Buncher	0.0	-2	1.21	257	4.34/4.63	+3	-0.053
1 st cavity	+2	0.0	1.53	260	4.30/4.58	-75	-0.22
1 st cavity	-2	0.0	1.23	306	4.60/4.90	+78	+0.42
1 st cavity	0.0	+2	1.22	296	4.45/4.75	+106	-1.81
1 st cavity	0.0	-2	1.52	269	4.41/4.69	-102	+2.04
2 nd cavity	+2	0.0	1.63	269	4.41/4.70	+114	-1.94
2 nd cavity	-2	0.0	1.89	295	4.45/4.74	-117	+2.33
2 nd cavity	0.0	+2	1.18	288	4.42/4.71	+85	-1.47
2 nd cavity	0.0	-2	1.41	277	4.45/4.73	-84	+1.63

d) Gun Parameter Variations

To evaluate the maximum operational flexibilities, the injector performance under different gun operating conditions has been investigated. These conditions include the voltage V_0 (keV), the field gradient E_0 (MV/m) at the cathode, the laser pulse length $4\sigma_L$ (ps) and the diameter d_0 (mm) of the active cathode area. The results are shown in Table 5. The low gradient of 6 MV/m was obtained by increasing the cathode-anode gap but holding the cathode and anode shapes unchanged. Low-gradient operation would be favorable for avoiding vacuum breakdown and cathode poisoning. It is seen that the design will function over a quite wide range of operating conditions.

Table 5 Gun Parameter Variations

V_0	E_0	$4\sigma_L$	d_0	$4\sigma_L$	$4\sigma_E$	$\epsilon_{nz}/\epsilon_{ny}$
500	10	100	3	0.96	290	4.44/4.73 (baseline)
500	10	60	3	2.00	109	3.65/3.85
500	10	60	5	1.54	118	3.78/3.97
500	10	100	5	0.79	287	4.07/4.44
400	8	100	3	1.24	272	5.32/5.02
400	8	60	5	0.91	260	6.12/6.08
500	6	100	3	0.91	330	6.49/6.12

e) Emission Phase Fluctuations

Emission of electrons is controlled by the laser pulses regularly illuminating the photocathode. Arrival time spread $\delta\phi_0$ (deg.) of the laser pulses will cause bunch-to-bunch energy spread δE_m and bunch-to-bunch centroid phase shift $\delta\phi_m$. As is shown in Table 6, the effects on both mean energy and centroid phase are negligible.

Table 6 Emission Phase Fluctuations

$\delta\phi_0$	$4\sigma_L$	$4\sigma_E$	$\epsilon_{nz}/\epsilon_{ny}$	δE_m	$\delta\phi_m$
0	0.96	290	4.44/4.73	0	0 (baseline)
+2	1.06	276	4.50/4.80	-14	+0.039
-2	0.94	303	4.32/4.61	+15	-0.029

f) Space Charge Effects

The setup procedure is one of our major concerns. To investigate the possibility of using a low-current beam to guide the injector to its full-charge (120 pC) operation, an integrated simulation was conducted, in which the space charge was simply turned off, in the case of 400-kV gun voltage, 60-ps laser pulse length and 5-mm cathode diameter[9].

In this specific case, the bunch length changes from 0.96 ps with space charge on to 1.92 ps with space charge off. This is because the system parameters are for a matched space-charge-dominated bunch in longitudinal phase space. The normalized rms emittance $\epsilon_{nz}/\epsilon_{ny} = 3.53/3.47$ mm mrad with space charge on or 0.66/0.66 mm mrad with space charge off, at the exit of the gun. $\epsilon_{nz}/\epsilon_{ny} = 6.12/6.08$ mm mrad with space charge on or 2.19/1.83 mm mrad with space charge off, at the exit of the chicane.

Our numerical calculations show that on a step-by-step basis, a lower current beam can be used to guide the injector to its full-charge operation, which will greatly simplify the setup procedures.

IV. SUMMARY

Extensive careful integrated computer simulations have demonstrated that our injector design will perform beyond the specifications over a quite wide range of operating conditions.

REFERENCES

1. J. Bisognano *et al.*, *Nucl. Instrum. Methods* A318, 216 (1992).
2. G. R. Neil *et al.*, *ibid.*, p. 212.
3. C. K. Sinclair, *ibid.*, p. 410.
4. P. Liger *et al.*, *ibid.*, p. 290.
5. T. Raubenheimer, Workshop on Fourth Generation Light Sources, SSRL, 263 (1992).
6. A. M. Sessler *et al.*, *Phys. Rev. Lett.* 68, 309 (1992).
7. K. T. McDonald, *IEEE Trans. ED*, 35, 2052 (1988).
8. H. Liu, to be published.
9. H. Liu, CEBAF-TN-93-009.